Article:
(2021) Interaction between filaments and ICRF in the plasma edge. Nuclear Materials and Energy. 100941. ISSN 2352-1791

https://doi.org/10.1016/j.nme.2021.100941

Nuclear Materials and Energy 26 (2021) 100941

Contents lists available at ScienceDirect

Nuclear Materials and Energy

journal homepage: www.elsevier.com/locate/nme

Interaction between filaments and ICRF in the plasma edge

W. Zhang [a,*], W. Tierens [a], V. Bobkov [a], A. Cathey [a], I. Cziegler [b], M. Griener [a], M. Hoelzl [a], O. Kardaun [a], the ASDEX Upgrade Team[1], the EUROfusion MST1 team[2]

[a] Max-Planck-Institut für Plasmaphysik, Garching, Germany
[b] University of York, York, Northern Ireland, United Kingdom

A B S T R A C T

Ion Cyclotron Range of Frequencies (ICRF) heating is a standard heating method for magnetic confinement fusion devices. ICRF waves can interact with filaments in the scrape-off layer (SOL) and induces a series of important phenomena. Understanding their interaction and the related physics is essential to the success of ICRF heating and plasma confinement. This paper is a review paper summarizing the recent progress in understanding of interaction between filaments and ICRF in the plasma edge and presents some key experimental and simulation results. In particular, the influence of RF convective cells on filament transport and the influence of filament on RF wave scattering, energy spectrum density, power redirection and wave mode conversion are discussed in detail. Most results shown in the paper make use of the published work, and some new results about mode conversion are also present.

1. Introduction

Radio-frequency (RF) heating with waves in the Ion Cyclotron Range of Frequencies (ICRF) has been widely used in nowadays magnetic confinement fusion devices. It is also planned for future fusion machines, such as ITER. Filaments are coherent structures of enhanced plasma pressure relative to the background plasma in the scrape-off layer (SOL), and carry a large fraction of plasma particles and energy across confining magnetic field lines. The ICRF fields can influence the transport of filaments in the SOL while filaments can also influence the propagation and absorption of ICRF waves. Understanding their interaction will not only be important to understand new physics in the SOL, but can also be vital to improve ICRF heating and plasma performance.

ICRF wave fields influence filaments in the SOL by driving convective E × B drifts [1,2]. These drifts, also known as RF convective cells, are induced by spatial inhomogenous RF rectified sheath potential. It is observed with the gas puffing imaging diagnostic that the RF convective cells can poloidally stretch, distort and even break up the filaments [2]. The change of filament behavior can subsequently change the local plasma density as well as the local plasma transport at the locations of RF convective cells.

Filaments influence ICRF wave fields by scattering the ICRF waves. This is because the plasma dielectric properties in the filament are different to the background plasma since the filament density is significantly larger than the background plasma density. Integrated simulations [3,4] with JOREK [5] and RAPLICASOL [6] or BOUT++ [7] and RAPLICASOL show that ELMs can lead to poloidally inhomogeneous density and wave fields in the SOL. The scattering of ICRF wave depends nonlinearly on many parameters associated with a filament. In addition, filaments can redirect part of the RF power from the perpendicular direction to the parallel direction (parallel to the background magnetic field) as a result of rectification of antenna power spectrum [3] and mode conversion of fast wave to slow wave [8].

2. Influence of convective cells on filaments

ICRF can induce convective cells (i.e. convective E × B drifts) locally close to the antenna due to the spatial differential of RF enhanced sheath potential in the SOL. The RF enhanced sheath potential is caused by sheath rectifications on the antenna and nearby wall due to different accelerations of ion and electrons by parallel electric fields in the SOL. Slow wave with a significant $E_{\parallel}$ is often considered as the source of the RF sheath rectification. These RF convective cells are located within the antenna extent in the poloidal direction and elongated along magnetic field lines in the toroidal direction. To measure these convective cells, the diagnostics have to sit either very close to the antenna or at locations magnetically connected to the powered antenna. The convective drifts are often largest in the center of the convective cells, where the gradients

* Corresponding author.
E-mail address: wei.zhang@ipp.mpg.de (W. Zhang).
[1] see the author list of H. Meyer et al. 2019 Nucl. Fusion 59 112014.
[2] see B. Labit et al 2019 Nucl. Fusion 59 086020.

https://doi.org/10.1016/j.nme.2021.100941
Received 2 July 2020; Received in revised form 26 January 2021; Accepted 3 February 2021
Available online 17 February 2021

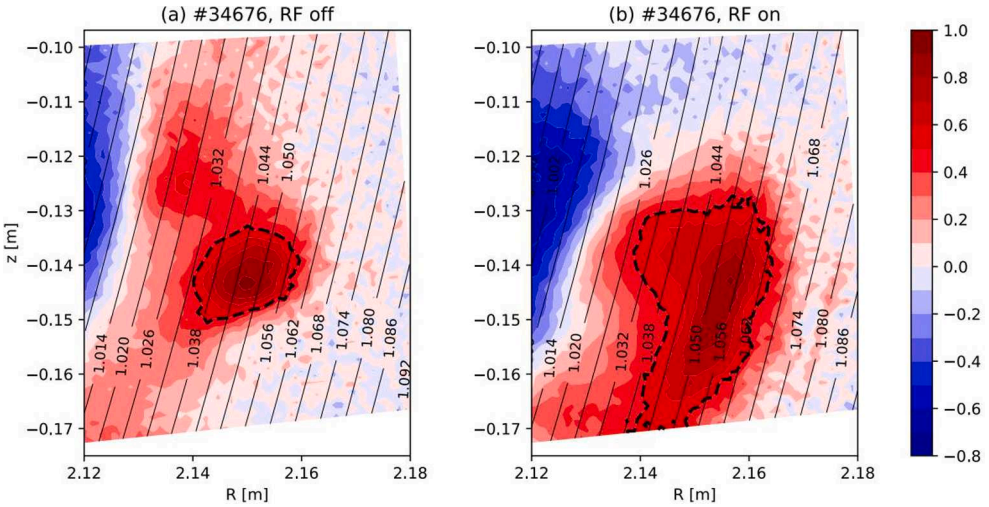

Fig. 1. Comparisons of correlation values for scenarios (a) without and (b) with RF convective cells in AUG discharge #34676. The GPI data in the time intervals (2.06, 2.061 s) and (3.032, 3.033 s) are used in the calculations for the cases without and with RF convective cells, respectively. The measured value at$\rho_{pol} = 1.05$ is used as a reference. Figure .
reproduced with permission from [2]

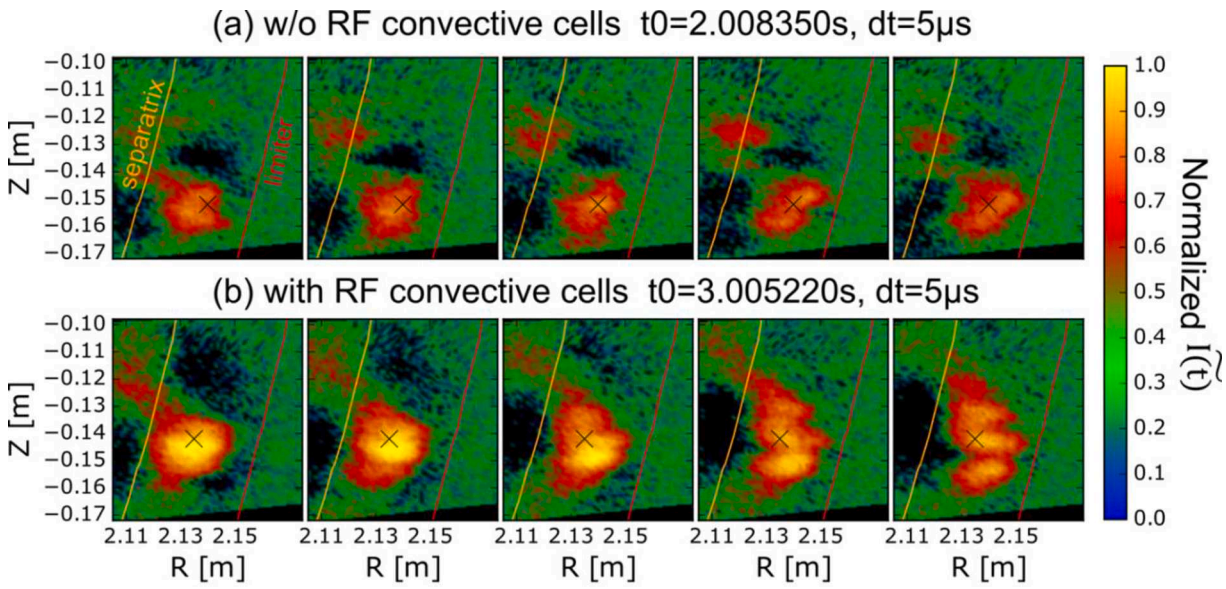

Fig. 2. Evolution of filaments for the cases (a) without and (b) with RF convective cells in discharge #34676. The cross mark is a reference position to visualize filament propagation. The time resolution of the GPI is 5μs. Figure .
reproduced with permission from [2]

of the RF rectified sheath potential are largest. Their magnitude can be in the same order as the diamagnetic drifts in the SOL (e.g. in the order of 1 km/s in ASDEX Upgrade (AUG) L–mode). Moreover, convective cells can connect to each other, allowing convective drifts to flow from one convective cell to another [1].

Previous studies show that when considering plasma in a steady state time scale (of the order of seconds), the RF convective cells not only cause density depletions in the center of convective cells, but can also leads to density accumulation at regions where the convective cells interact with the first wall [1]. Subsequently, the change of density just in front of the antenna can lead to a modification of ICRF power coupling and an enhanced plasma-wall interaction. When considering the plasma behavior in a turbulence time scale (of the order of microseconds), the convective cells can influence the transport of filaments locally.

To understand the influence of RF convective cells on filaments/blobs, multiple diagnostics, in particular the Gas Puff Imaging (GPI) located very close to the powered antenna, were used to measure the dynamics of filaments for cases without and with RF convective cells in AUG L-mode plasma. In these two cases, the first case uses ~ 0.6 MW ECRH (Electron Cyclotron Resonance Heating) power and the second case uses the same amount of ICRF power, corresponding to the cases without and with RF convective cells, respectively. All other plasma parameters are kept the same. It is found that the RF convective cells can stretch, distort and even break up the filaments poloidally [2]. An example of poloidal stretching of filaments is shown in Fig. 1. Since the fluctuation power in the far SOL is dominated by filaments, the correlation pattern is a measure of an average filament shape, i.e. filament cross-section. The contour of the highly (>0.5) correlated region shows roughly a circular shape for the case for the case without RF convective cells. In contrast, it has a highly poloidal stretched shape for the case with RF convective cells. This is a direct evidence of filament distortion and stretching by RF convective cells.

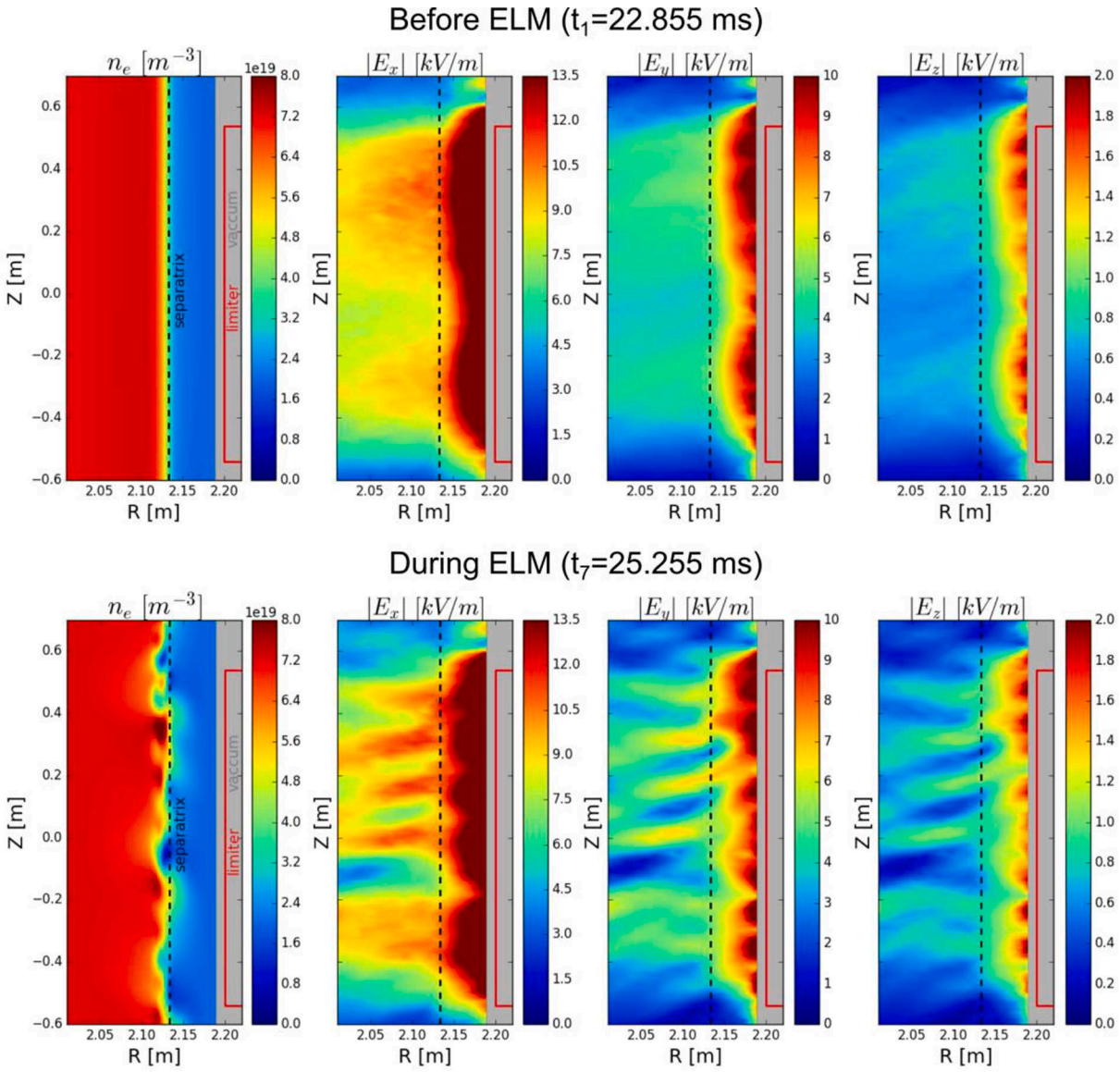

Fig. 3. Comparisons of SOL density and different components of wave electric fields for the cases before and during ELM. Figure reproduced with permission from [3]. The 3D density calculated by JOREK is reproduced from [11].

Beside this, the RF convective cells can also poloidally break up the filaments. Such an example is demonstrated in Fig. 2. It can be seen that in the case without RF convective cells, the filament transports radially outward with just a gradual change of shape. In the case with RF convective cells, the filament is firstly poloidally stretched and then it is torn apart into smaller pieces as it moves further outward. Whether the filament is only poloidally stretched or can be further broken up depends of the magnitude of the shear flow. Here the shear flow is developed since the radially inner part of RF convective drifts are in the upward direction while the diamagnetic drifts are in the downward direction. From the statistical analysis of more than 1000 complete filament events, it is found that the events of poloidal stretch and splitting of the filament for the cases with RF convective cells are much more abundant than the case without RF convective cells [2].

Moreover, the generated shear flow can lead to filament stopping [9], which is expected to facilitate divertor detachment [2]. These results suggest that externally generating shear flow in the SOL can be considered as a method to modify filament transport and control the radial transport of heat fluxes.

3. Influence of filaments on RF wave propagation

The RF convective cells can influence the transport of filaments in the SOL, while the filaments in return can influence the propagation of ICRF waves. This is because the presence of filaments changes the local plasma dielectric properties and thus the wave dispersion relation. Subsequently, the wave propagation in the SOL is influenced.

To understand how the filaments influence RF wave propagation, experimentally, the 2D Mie scattering analytical model [10] and the 2D/3D COMSOL models are developed to calculate the perturbation of wave fields by filaments [3]. In these models, the filaments are assumed to be infinitely long and aligned with the magnetic field lines in the toroidal direction, and have circular cross-sections in the polodial cross-section. Plane waves are used in the 2D models while realistic antenna geometries and power spectrum are defined in the 3D model. The simulation results indicate that the level of RF wave scattering increases nonlinearly as the filament density and filament radius increases before getting saturated. In the presence of one filament, a scattering cone starting from the center of the filament is developed. In the presence of multiple filaments, poloidal distributed and radially elongated stripe structures

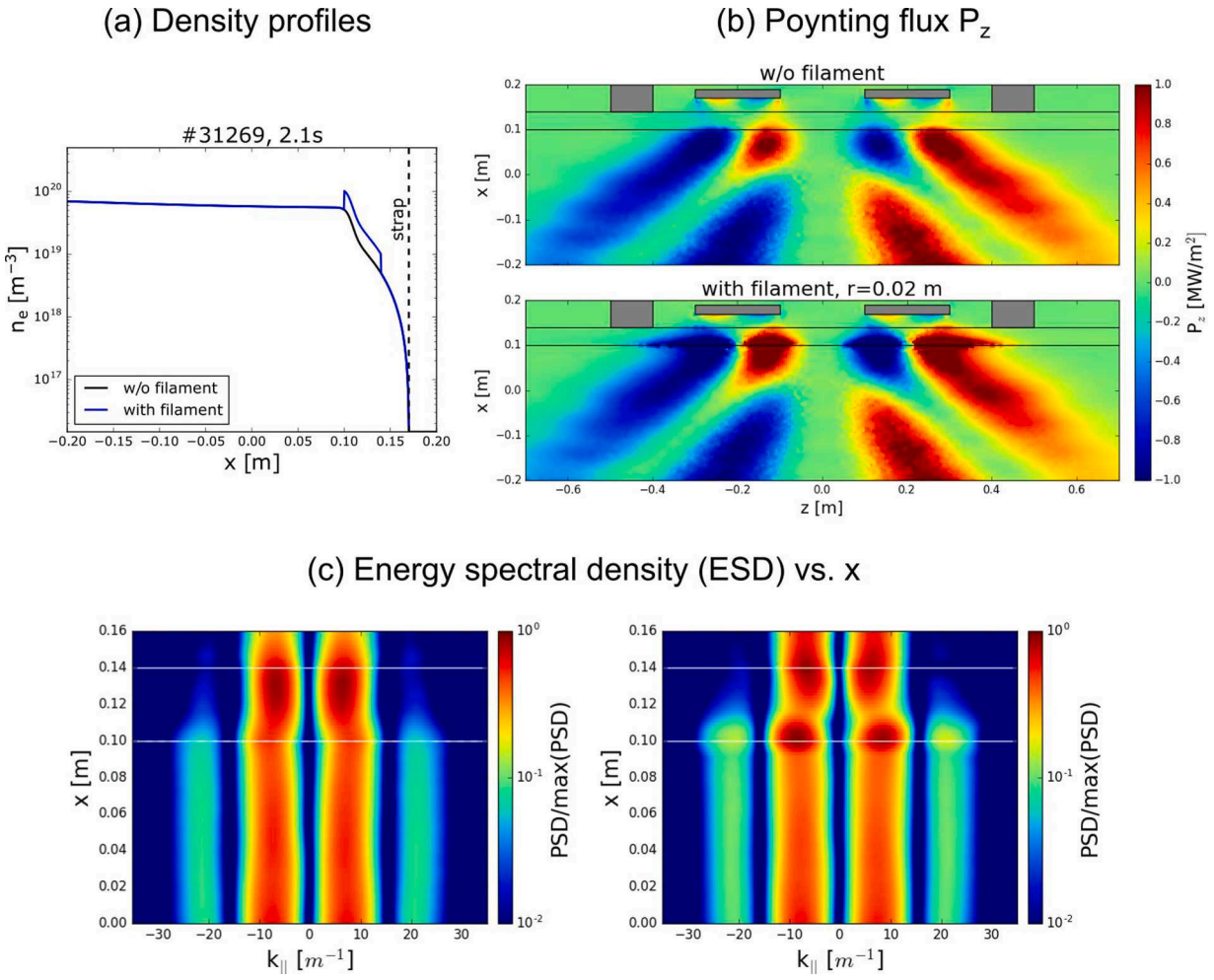

Fig. 4. 3D COMSOL simulations with AUG experimental density profiles. (a) Density profiles used for the cases without (black line) and with (blue line) a filament. (b) z component of the time averaged Poynting flux in the x-z plane (y = 0.0 m) for the cases without and with a filament. (c) Normalized Energy spectral density (ESD) in the × direction without and with filament. The ESD is normalized to the largest value of the two cases. The horizontal lines depict the locations of the filament. Figure . (For interpretation of the references to color in this figure legend, the reader is referred to the web version of this article.)
reproduced with permission from [3]

with enhanced and reduced electric fields are developed. The scattering cones become less obvious and the scattering effect becomes more global as the number of filaments or the distance between filaments increases [3].

A more realistic description of the density fluctuations in the SOL is necessary in order to obtain a more realistic wave scattering. For this, the turbulence code BOUT++ [7] or the MHD code JOREK [5] is used to calculate the 3D turbulent SOL density, which are then used in the 3D antenna code RAPLICASOL to calculate the 3D perturbed wave fields and Poynting fluxes. In particular, cases before and during the burst of ELMs are studied. An example is shown in Fig. 3, where the JOREK code is used to calculate the 3D density. It is shown that during ELMs, the SOL density become quite inhomogeneous poloidally. The density perturbation in the filaments is in the level of ~ 80%, leading to a global perturbation of electric field in the level of $\delta E_x \sim 40\%$, $\delta E_y \sim 80\%$ and $\delta E_z \sim 80\%$, respectively. Due to the mutual influence of multiple density filaments, radially elongated but poloidally distributed stripe structures with regions of enhanced and reduced wave fields develop in the SOL. This finding is consistent with the 2D COMSOL simulations in which multiple filaments are taken into account. In addition, the stripe structures originating from the SOL and can extend radially into the core plasma. It is expected that due to this mechanism, the RF heating in the resonance layer will be poloidally inhomogeneous, and the radial heat deposition profile will be affected. To understand the influence of RF wave scattering on the RF power absorption in the plasma core, we plan to use the 3D ELM density calculated by JOREK in the 3D HIS-TORIC code [12] to estimate the modifications of wave absorption in the plasma core. This work is foreseen in the near future.

Beside the influence on RF wave scattering, ELMs can also influence the ICRF power coupling in the SOL. On one hand, more power is reflected in the transmission line and less power is emitted by the antenna, as the impedance matching condition is changed due to the modification of SOL density profiles during ELMs. On the other hand, the antenna loading resistance becomes larger, since the increase of SOL density leads to a decrease of the width of the evanescent layer. However, the former effect always changes the coupling more significantly than the latter effect. Thus, a combination of the two competing effects leads to a decrease of coupled power from the antenna to the plasma during ELMs.

4. Influence of filaments on power redirection

Filaments not only cause RF waves scattering, but can also change the power spectrum locally and redirect part of the power flow from the perpendicular direction (perpendicular to the magnetic field) to the parallel direction. To understand this effect, a 3D COMSOL model using realistic power spectrum and experimental density has been built [3]. Cases without filaments and with a filament have been compared. In both cases, the magnetic field is $B_0 = 2$ T and the ICRF frequency

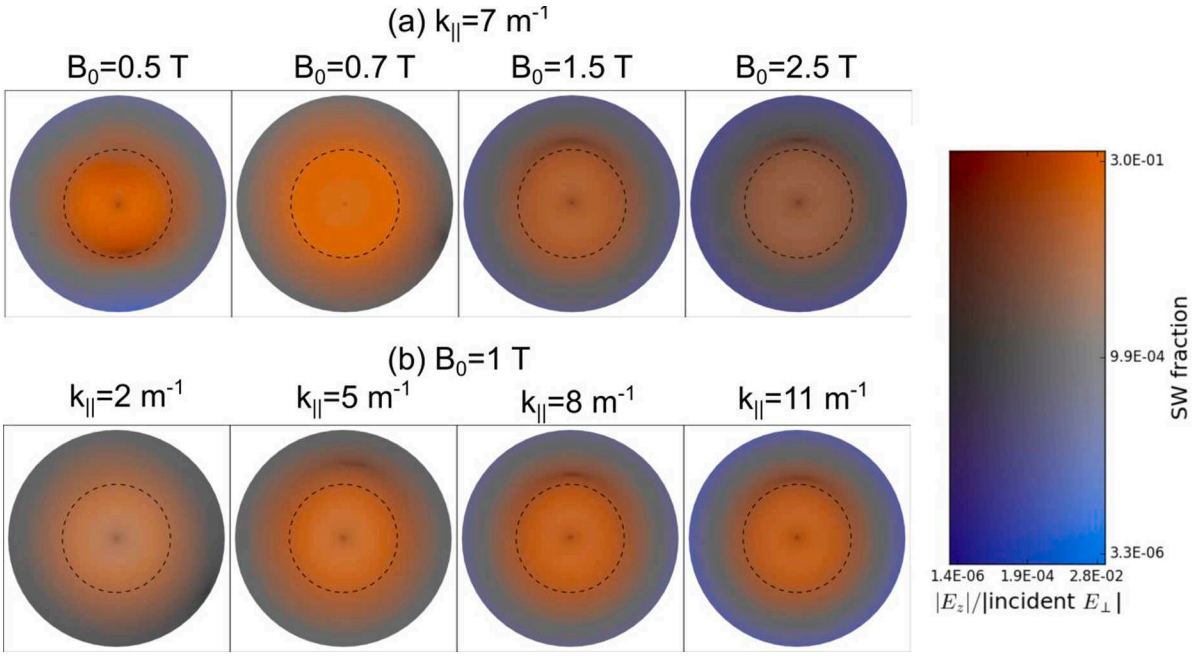

Fig. 5. Filament induced mode conversion with (a) constant$k_{||} = 7m^{-1}$ but different B_0; (b) constant$B_0 = 1$ T but different $k_{||}$. The black dashed circle depicts the boundary of the filament. The radius of the filament is 1 cm.

is$f_{ICRF} = 36.5$ MHz. Cold plasma without collision is assumed in the simulations. Perfect Matching Layers (PMLs) are used as boundary conditions. In AUG, the typical density ratio between the filament and the background plasma ($n_{e,F}/n_{e,B}$) is in the range of 2–3, and the typical filament radius (r_F) is in the range of 5 mm – 4 cm [13-15]. In this section, typical filament parameters of$n_{e,F}/n_{e,B} = 2$ and$r_F = 0.02$ m are used. The density profiles used in the simulations are shown in Fig. 4(a).

From the analysis of the electric fields and Poynting fluxes, it is found that part of the power carried by the fast wave can be redirected from the radial direction to the parallel direction, as shown in Fig. 4(b). The redirected power flux is in the level of 1 MW/m^2. For a realistic density profile, the toroidal extension of the redirected parallel power flux is in the level of a few decimeters. When the filament density is much larger than the background density (for instance$n_{e,F}/n_{e,B} = 5$), the toroidal extension of the redirected parallel power flux can reach the level of meters. This power redirection is caused by the increased magnitude of the perpendicular electric and magnetic fields in the filament. The increase of the wave fields subsequently leads to an increase of Energy Spectrum Density (ESD) in the filament. Here ESD=$\left| \int_{-\infty}^{\infty} e^{-2\pi i k x} E(x) dx \right|^2$. A comparison of the ESD for the cases without and with filament is shown in Fig. 4(c). It is indicated that ESD remains roughly the same outside the filament in both cases, but changes significantly in the filament. The ESD magnitude of both the primary wavenumber$k\| = 8$ m^{-1} and the secondary wavenumber$k\| = 21$ m^{-1} become obviously larger in the radially outward half of the filament.

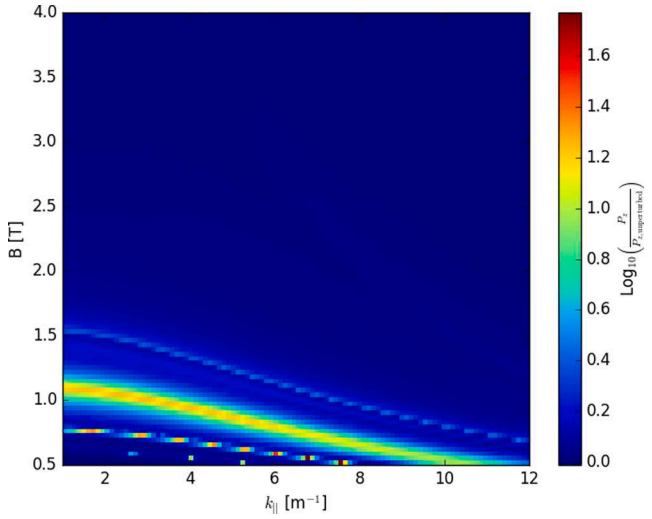

Fig. 6. The ratio between perturbed parallel power flux P_z (cases with filament) and the unperturbed power flux $P_{z,unperturbed}$ (cases without filament) as a function of $k_{||}$ and B_0. This figure shows under which condition (i.e. with which $k_{||}$ and B_0 values), the power ratio of the parallel power flux (i.e. the power redirection effect) is most significant. The bright wide orange line represents the main resonance condition where intensive fast to slow wave mode conversion happens. (For interpretation of the references to color in this figure legend, the reader is referred to the web version of this article.)

The parallel redirected power can be as large as 1 MW/m^2, and it can be focused on a small region of the wall, with a cross-section similar or smaller than the cross-section of the filament. However, this redirected power cannot be directly deposited on the wall (limiter or divertor) surface because of wave reflection. The resistive losses on the antenna limiters due to induced currents can be increased by an order of magnitude, to a level $\sim 10^3 W/m^2$. But it is still too small to cause any damages to the limiter. Other than this, the slow wave generated by filament assisted mode-convection together with sheath rectification at the wall (limiter or divertor) surface may cause significant impurity sputtering at the wall. This mechanism will be investigated in the near future.

5. Influence of filaments on wave mode conversion

At the filament surface, where the density gradient is steep, mode conversion from the incident Fast Wave to the usually evanescent slow wave (SW) occurs. Under certain circumstances, notably high–harmonic heating with low $k_{||}$ [8], this mode conversion can be very strong, leading to large parallel electric fields (associated with the mode-converted slow wave) near the filament and/or large parallel power flow along the filament. This is another mechanism which causes parallel power redirection, in addition to the mechanism mentioned in section 4.

Within an analytical solution for wave scattering at filaments whose density is a piecewise constant function of the filament radius in cylindrical coordinates centered on the filament [10], it is possible to clearly distinguish the electric field due to the Fast wave and that due to the Slow Wave, and we may define the "SW fraction" as |E due to SW|/(|E due to FW|+|E due to SW|). Strong mode conversion depends on the filament radius, parallel wave number, antenna frequency, ion cyclotron frequency and ion to electron mass ratio [8], in which the ion cyclotron frequency depends on the background magnetic field. In our studies, typical plasma and filament parameters are considered, and the parallel wave number and background magnetic field are varied to understand their influence on mode conversion. A Gaussian density is defined for the filament, where the maximum filament density at the filament center is set as two times of the background plasma density, and the filament radius ($r_F = 1$ cm) is defined as from the filament center to the boundary where the density is 1% higher than the background density. The ICRF heating frequency is$f_{ICRF} = 36.5$ MHz and the background plasma density is$n_{e,B} = 5 \times 10^{18} m^{-3}$. Lossless cold plasma model is used to calculate the wave dispersion. All quantities (filament and wave) are assumed to be constant in the direction along filament. Fig. 5 shows the electric field near the filament, color-coded according to the slow wave fraction, so that the mode conversion from the incident (blue) fast wave to the mode-converted orange slow wave is clearly visible. For the cases with constant$k_{||} = 7m^{-1}$ but different B_0, the mode conversion is largest for the case with$B_0 = 0.7$ T. For the cases with constant$B_0 = 1$ T but different $k_{||}$, the mode conversion is largest for the case with$k_{||} = 5m^{-1}$. These are consistent with the high parallel power flux (P_z) pattern shown in Fig. 6.

An example of the parallel power flux caused by mode conversion is shown in Fig. 6, where each point corresponds to one simulation case (i.e. independent case such as the ones in Fig. 5), and the whole figure is a combination of the scan of $k_{||}$ and B_0. The results show that the parallel power flux along a Gaussian filament is ~ 10 times larger than that in the unperturbed case, but only in a narrow band at low magnetic field, i.e. high-harmonic heating. The main resonance in Fig. 6 is in qualitative agreement with the analytic result for filaments with discontinuous density in [8], for resonances with azimuthal mode number 1. In addition, two thinner resonances, likely corresponding to different azimuthal mode numbers, are also visible. The peak in power flux corresponds to a resonance in a dispersion relation. However, this is not a dispersion relation that one could easily write down because a Gaussian density profile (more realistic than constant density) is assumed for the filament. Even for a constant filament density, the dispersion relation is too complicated to formulate. Nevertheless, further efforts will be spent to investigate an analytical formula to express the resonance condition with good approximation.

6. Conclusions

Some recent progress in the study of the interaction between filaments and ICRF in the plasma edge is summarized in the paper. In particular, the influence of RF convective cells on filament transport as well as the scattering of RF waves, power redirection and mode conversion by filaments in the SOL is discussed in detail. It is found that the RF induced convective cells can poloidally distort, stretch and break up filaments and influence the local plasma transport in the SOL. The RF wave scattering depends on the filament size, filament density, number of filaments and distance between filaments. The mutual influence of multiple filaments induces poloidally distributed and radially extended stripe structures in the wave fields and Poynting fluxes. In addition, the wave fields inside the filament are locally increased, leading to a change of energy spectrum density and a redirection of power flow from the perpendicular direction to the parallel direction (parallel to the magnetic field). Significant mode conversion of fast wave to slow wave can happen at resonance conditions, especially when the magnetic field is low.

Our studies greatly improve our understanding on this topic. They are not only important for developing methods to better control filament transport in favourable ways, but also essential for improving RF heating efficiency and reducing undesired plasma-wall interactions in fusion devices. Further work with more quantitative comparisons between experiments and simulations will shed more light on these.

Declaration of Competing Interest

The authors declare that they have no known competing financial interests or personal relationships that could have appeared to influence the work reported in this paper.

Acknowledgements

This work has been carried out within the framework of the EUROfusion Consortium and has received funding from the Euratom research and training programme 2014-2018 and 2019-2020 under grant agreement No 633053. The views and opinions expressed herein do not necessarily reflect those of the European Commission.

References

[1] W. Zhang, et al., Plasma Phys. Control. Fusion 58 (2016), 095005.
[2] W. Zhang, et al., Nucl. Fusion 59 (2019), 074001.
[3] W. Zhang, et al., Nucl. Fusion 60 (2020), 096001.
[4] W. Zhang, et al., "Influence of ELMs on ICRF" *The 23rd Topical Conference on Radiofrequency Power in Plasmas (RFPPC)*, Hefei, China, 2019.
[5] G.T.A. Huysmans, et al., Nucl. Fusion 47 (2007) 659–666.
[6] J. Jacquot, et al., AIP Conf. Proc. 1689 (2015), 050008.
[7] B.D. Dudson, et al., Comput. Phys. Commun. 180 (2009) 1467–1480.
[8] W. Tierens, et al., Phys. Plasmas 27 (2020), 010702.
[9] P. Ghendrih, et al., J. Nucl. Mater. 390–91 (2009) 425–427.
[10] A.K. Ram, et al., Phys. Plasmas 23 (2016), 022504.
[11] Cathey Cevallos A. et al 2020 "Non-linear magnetohydrodynamic simulations of type I edge localized mode cycles intokamak plasmas and their underlying triggering mechanism", Submitted to Physical Review Letters.
[12] S. Shiraiwa, et al., Nucl. Fusion 57 (2017), 086048.
[13] G. Birkenmeier, et al., Plasma Phys. Controlled Fusion 56 (2014), 075019.
[14] Carralero D. et al 2018 Nuclear Fusion 58.
[15] D. Carralero, et al., Nucl. Fusion 54 (2014), 123005.